New Journal of Physics
The open-access journal for physics

Local and global deformations in a strain-stiffening fibrin gel

Qi Wen[1,2], Anindita Basu[1], Jessamine P Winer[2], Arjun Yodh[1,3] and Paul A Janmey[1,2,3]

[1] Department of Physics and Astronomy, University of Pennsylvania, Philadelphia, PA 19104, USA
[2] Institute for Medicine and Engineering, University of Pennsylvania, Philadelphia, PA 19104, USA
E-mail: janmey@mail.med.upenn.edu

New Journal of Physics **9** (2007) 428
Received 31 May 2007
Published 30 November 2007
Online at http://www.njp.org/
doi:10.1088/1367-2630/9/11/428

Abstract. Extracellular matrices composed of filamentous biopolymers like collagen and fibrin have viscoelastic properties that differ from those of rubberlike elastomers or hydrogels formed by flexible polymers. Compared to flexible polymer gels, filamentous biopolymer networks generally have larger elastic moduli, a striking increase in elastic modulus with increasing strain, and a pronounced negative normal stress when deformed in simple shear. All three of these unusual features can be accounted for by a theory that extends concepts of entropic elasticity to a regime where the polymer chains are already significantly extended in the absence of external forces because of their finite bending stiffness. An essential assumption of the theories that relate microscopic structural parameters such as persistence length and mesh size of biopolymer gels to their macroscopic rheology is that the deformation of these materials is affine: that is, the macroscopic strain of the bulk material is equal to the local strain within the material at each point. The validity of this assumption for the dilute open meshworks of most biopolymer gels has been experimentally tested by embedding micron diameter fluorescent beads within the networks formed by fibrin and quantifying their displacements as the macroscopic samples are deformed in a rheometer. Measures of non-affine deformation are small at small strains and decrease as strain increases and the sample stiffens. These results are consistent with the entropic model for non-linear elasticity of semiflexible polymer networks and show that strain-stiffening does not require non-affine deformations.

[3] Authors to whom any correspondence should be addressed.

PII: S1367-2630(07)51643-5

Contents

1. Introduction

Networks of cytoskeletal filaments like F-actin and vimentin, and extracellular matrices like collagen and fibrin have viscoelastic properties that are very different from those of rubberlike elastomers or hydrogels formed by flexible polymers like polyacrylamide. Biopolymer gels generally have much higher shear moduli at very low volume fractions compared to hydrogels formed by synthetic polymers [1]; they often exhibit a striking increase in elastic modulus with increasing strain over a range of strains where flexible polymer gels maintain a constant stiffness [2, 3]; and they show a pronounced negative normal stress when deformed in simple shear that is not reported for other elastic materials [4]. The unique rheology of biological gels and tissues is thought to be due to the structure of most biopolymer filaments, which are significantly thicker (ranging from 6 to 25 nm in diameter) than synthetic polymers, and are much stiffer, with persistence lengths ranging from 300 nm [5] to 20 μm [6], and are therefore not approximated adequately as either rodlike or flexible molecules. All three of these unusual features: high modulus at low volume fraction, strain-stiffening, and negative normal stress can be accounted for by a theory that extends concepts of entropic elasticity to a regime where the polymer chains are already significantly extended in the absence of external forces because of their finite bending stiffness [7]. Alternative models can also account for some of these features [8]–[11], but whether a single alternative model predicts all three features of biopolymer gels is not yet determined.

An essential assumption of some theories that relate microscopic structural parameters such as persistence length and mesh size of biopolymer gels to their macroscopic rheology is that the deformation of these materials is affine: that is, the macroscopic strain of the bulk material is equal to the local strain within the material at each point. This affine assumption has been shown to be adequate for relatively dense rubberlike networks, but its validity for the dilute open meshworks of most biopolymer gels has not yet been extensively tested. One recent

study of crosslinked actin networks reported significant non-affinity at shear strains between 10 and 30% [12], but systematic studies relating affinity measures to strains below and within the range of strain-stiffening have not yet been reported. At a length scale below that of the network mesh size, generally in the range of 100–500 nm, this assumption must necessarily break down, but whether it holds for larger distances that might be biologically significant is not known. Some simulations of non-thermal two-dimensional (2D) networks of filaments show that the local strains become highly non-affine at moderate strains (10–50%) where strain stiffening becomes significant [10], and the change in network geometry and non-affinity is essential to the mechanism of strain stiffening in some models. Even at small strains isotropic materials such as the randomly crosslinked networks of the cytoskeleton and extracellular matrix are necessarily non-affine and simulations, mostly in 2D, show that finite measures of non-affine deformation decay as strains increase [13]. The magnitude of non-affinity depends strongly on molecular parameters such as filament length, concentration, density of crosslinks and geometry of networks and is not yet possible to infer from the theory alone.

In order to determine whether the assumption of affine deformation is valid over a range of strain where the elastic response of a biopolymer gel is highly non-linear, we embedded micron-sized beads in a fibrin gel with mesh sizes ranging from 200 to 500 nm and visualized the movement of multiple beads within the network as it was deformed in a range of strain amplitudes over which the elastic modulus increased significantly. The experiments were made with fibrin clots because these materials are intrinsically crosslinked and more reproducible than networks formed by cytoskeletal proteins with their associated crosslinkers [14]–[16]. The stiffness, diameters and mesh size of fibrin filaments and gels very closely resemble those of intermediate filaments, and therefore, the findings in this system are likely to be applicable to semiflexible biopolymer networks in general.

2. Experimental methods

2.1. Sample preparation

Lyophilized fibrinogen [17] and thrombin [18] prepared from salmon blood plasma were provided by Sea-Run Holdings, Inc. (South Freeport, ME). Fibrinogen was rehydrated and dialyzed against 50 mM Tris, 150 mM NaCl, pH 7.4 at a concentration of 20 mg ml^{-1} and diluted in the same buffer to the target concentration. Thrombin was rehydrated in 50 mM Tris, 1 M NaCl, pH 7.4 at a concentration of 1500 NIH U m^{-1}. Fibrin gels were made by addition of 1 NIH U ml^{-1} thrombin to 2.5 mg ml^{-1} fibrinogen polymerized *in situ* between the rheometer plates. Under these conditions, fibrin makes optically clear gels containing a mixture of single protofibrils with diameters of 10 nm and persistence length of 500 nm, and thin bundles of protofibrils with diameters below 15 nm, as measured by atomic force microscopy. Fluorescent beads with a mean diameter of 1 μm were purchased from Molecular Probes (Invitrogen Corp., Eugene, Oregon, USA), with an excitation wavelength of 580 nm and an emission wavelength of 605 nm. To prepare gels with embedded fluorescent beads, a stock solution of beads was diluted into the thrombin solution before fibrinogen was added. The concentration of beads was adjusted empirically to produce a sufficient bead density to allow tracking of multiple beads in the observation volume without the overlapping of fluorescence intensities from adjacent beads.

2.2. Atomic force and scanning electron microscopy

Fibrin fibers were imaged by a multimode atomic force microscope (Digital Instruments, Inc., Santa Barbara, CA). Samples for AFM imaging were prepared on a mica surface. Before applying the sample, the mica surface was submerged in a $0.1\,\mathrm{mg\,ml^{-1}}$ poly-lysine solution for 30 min. Blowing away the poly-lysine solution by a flow of nitrogen resulted in a mica surface with a thin layer of poly-lysine. A drop ($\sim 3\,\mu$l) of $100\,\mathrm{NIH\,U\,ml^{-1}}$ thrombin was then applied on the poly-lysine treated mica surface. After incubating for 2 min, a drop ($\sim 50\,\mu$l) of $0.5\,\mathrm{mg\,ml^{-1}}$ fibrinogen in T7 buffer was added to the thrombin solution with gentle mixing. After incubating the sample for 10 min, the sample was flushed with DI water and then dried with nitrogen. This step generates a mica surface with adsorbed fibrin fibers. The sample was then imaged on a Multimode AFM using contact mode.

For scanning electron microscopy, a $2.4\,\mathrm{mg\,ml^{-1}}$ fibrinogen solution in T7 buffer was gelled at room temperature using 20 mM $CaCl_2$ and $1.5\,\mathrm{U\,ml^{-1}}$ thrombin. The SEM sample was fixed, dehydrated, critical point dried and coated with gold/palladium as described previously [19]. The images were taken on a Philips XL20 scanning electron microscope (Philips Electron Optics, Eindhoven, The Netherlands) in the electron microscopy facility at the Department of Cell Biology University of Pennsylvania, PA, USA.

2.3. Rheology

Rheologic measurements of fibrin networks were performed on a stress-controlled Bohlin Gemini rheometer (Malvern Instruments, UK). A 4° cone was used as the upper plate. To prevent sample drying, a solvent trap was applied to cover the sample. The shear storage modulus G' was measured by oscillatory shear strain at a frequency of 0.1 Hz and a maximal strain amplitude of 1% as a function of time during polymerization. Oscillatory amplitude sweep measurements at a frequency of 0.5 Hz were carried out to measure the non-linear elasticity of fibrin networks with strain values varying from 1 up to 160%. G', G'', the shear loss modulus and the second normal stress difference were measured as functions of strain.

2.4. Non-affinity measurements

Local deformations in the gels were detected by measuring the displacements of fluorescent beads embedded in the gel using the set-up shown in figure 2(a). To visualize the fluorescent beads, a Nikon TE 200 microscope was mounted below the rheometer with the lower measurement plate replaced by a microscope glass slide mounted on a home built microscope stage. An extensional rod was built to bring the upper plate of the rheometer down to the microscope stage and enable the rheometer to apply stress to the gels. A 60× extra long working distance objective with a WD of 1.5–2.1 mm was controlled by a E-662 piezoelectric actuator (Physik Instrumente, Germany) to move up and down so that its focal point could sweep through the sample thickness. This arrangement enabled us to image beads at different depths within the sample. Positions of beads in the focal plan with shear on and off were recorded by a Hamamatsu CCD camera (C4742-95). Images were then processed using a Matlab routine, which determines the beads' positions with subpixel resolution [20], to quantify the displacements of beads with a resolution of 50 nm.

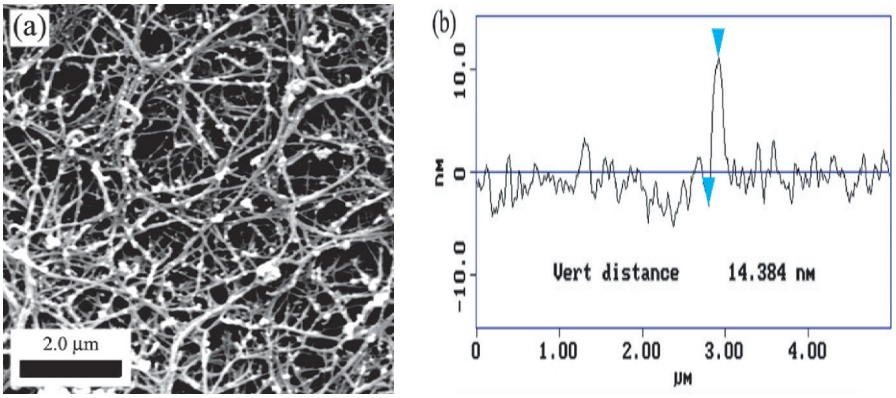

Figure 1. Visualization of fibrin network (a) SEM image of fibrin gel, (b) example line scan of AFM height image showing protofibril height as ∼14 nm.

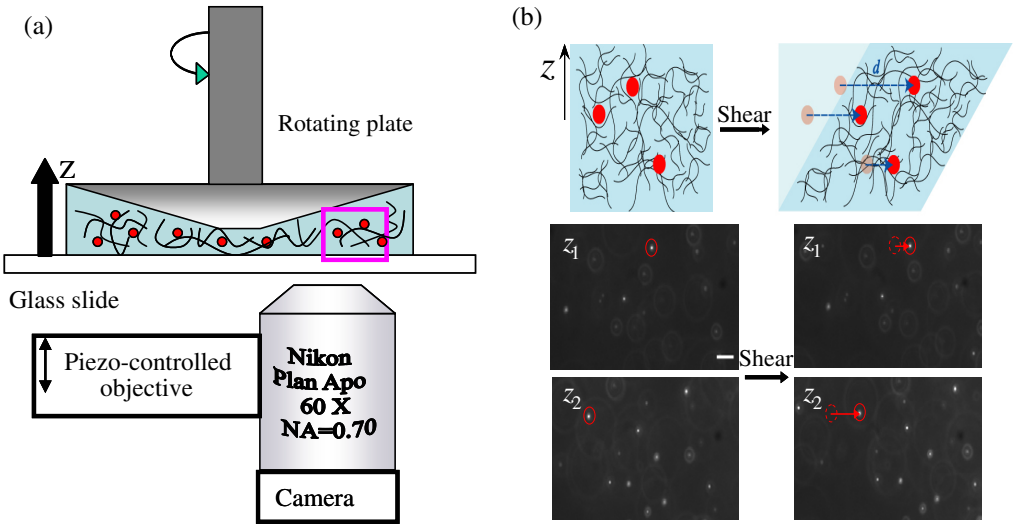

Figure 2. Schematic sketch of experimental system. (a) Diagram of experimental set-up. (b) Sketch of displacement of beads in polymer network and images of beads taken before and after the shear stress were applied. All of the four images have the same magnification. The scale bar in the upper left image represents 10 μm.

3. Results and discussion

3.1. Structure of fibrin gels and effect of embedded beads on fibrin viscoelasticity

For a 2.5 mg ml^{-1} fibrin gel, the mesh size is estimated to be about 200 nm from the previously determined values of mass to length ratio and diameter of the filaments [3]. This estimate is confirmed by the scanning electron micrograph shown in figure 1(a). The diameter of the fibrin strands is estimated from the height measurements using AFM of filaments adherent to a mica surface. As shown in figure 1(b), diameters range from approximately 10 to 20 nm, consistent

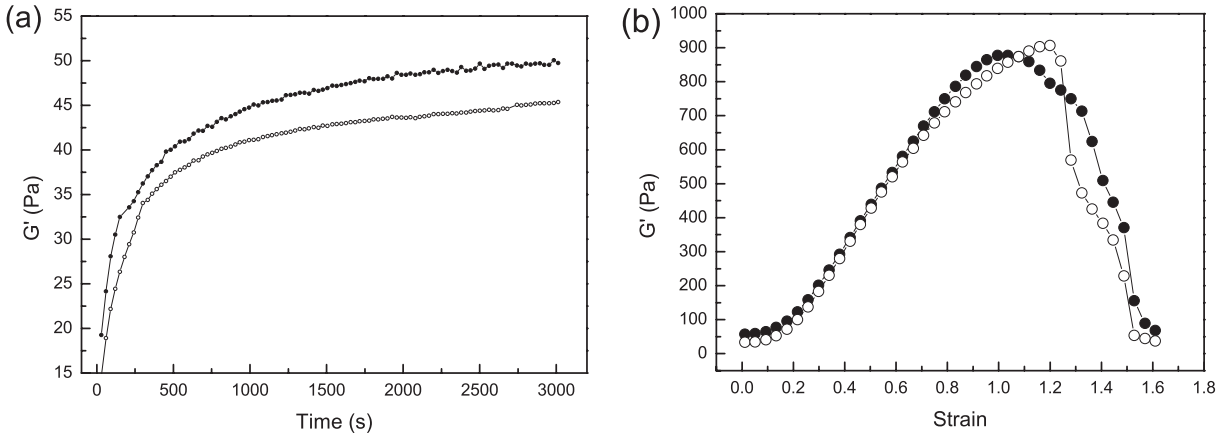

Figure 3. G' as functions of time and strain for gels with (empty circles) and without (solid circles) beads embedded. (a) Polymerization of fibrin leads to increase in G'. (b) Stiffness of gels increase with increasing strain values indicating the nonlinear elasticity of the gels.

with a network of fibrin protofibrils and very small protofibril bundles. The thickness of the salmon fibrin strands at physiological values of pH and ionic strength is significantly lower than that of fibrin formed from human or bovine fibrinogen as previously shown by turbidity measurements [17], and may account for the greater resistance of salmon fibrin to degradation in wound healing applications *in vivo* [21, 22].

The size of fluorescent beads was selected to be larger than the mesh size of the fibrin network so that their Brownian motion is suppressed. Viscoelastic properties of fibrin gels with embedded beads were compared to those without beads. In figure 3, G' increases as a function of time during polymerization. The added beads do not alter the polymerization rate, since the G' for gel with beads increases at the same rate as that for the gel without beads. The final G' values at 1% strain taken after 1 h for both types of gels were measured to be: 45 ± 5 Pa. These results suggest that the fluorescent beads are likely to act as tracers for fibrin gel displacements and do not form defects or additional crosslinks in the network that would alter the gel rheology.

3.2. Non-linear elasticity

As the strain values increase from 1 to 160%, the elastic modulus increases from approximately 50 Pa to a maximum value of 900 Pa at about 120% strain (see figure 3(b)). The strain sweep curves for gels with and without embedded beads are not statistically distinguishable, confirming further that the beads do not alter gel structure. The sharp decrease in G' at larger strains is possibly due to sample failure, i.e. network disruption or network detachment from the rheometer plates.

3.3. Negative normal stress

The second normal stress difference, which is in the direction perpendicular to the rheometer plate, has also been recorded. A negative normal stress, as has been reported for other biological gels [4], was also observed in the fibrin networks. Results in figure 5 show that the magnitude

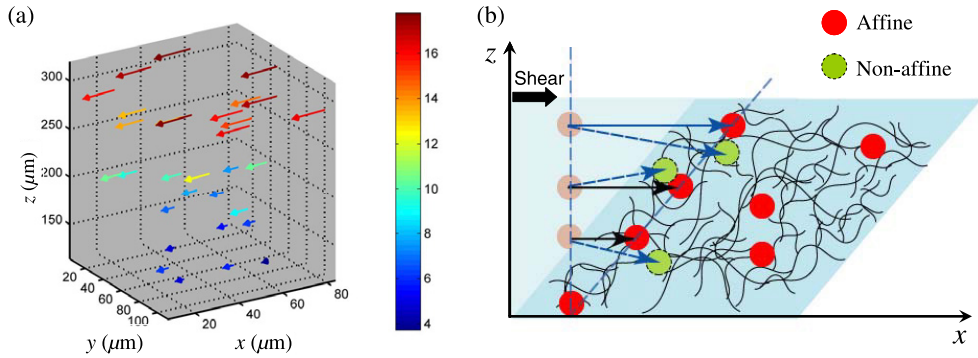

Figure 4. Sketch of non-affine deformation. (a) Measured displacement of beads in gel. Arrows in the plot represent the displacement vector for beads, with color indicating the magnitude of the displacement. (b) Sketch of non-affine deformation in the gel.

of normal stress increases as a function of strain and declines as the sample softens after rupture.

3.4. Displacement of beads in the gel

The microscope was able to record the displacement of beads in a 60 μm $\times$ 60 μm area. Within this small area, approximately 1 cm from the axis of rotation, the strain applied to the sample can be approximated as a unidirectional shear. Figure 4(a) shows the displacement of beads in a sample, where the direction of shear is taken as the direction of the x-axis. As z, the distance from the bottom surface up into the gel increases, the lateral displacement also increases approximately in a linear manner. As depicted in figure 4(b), the non-affine deformation can be characterized by the displacements along both the x- and z-axes. Displacement of the beads in the z-direction can be detected by monitoring the size of diffraction ring of the beads out of focus. Due to the large focal depth of the microscope objective, $\sim$500 nm, only z displacements larger than 500 nm can be detected. Within this limit, no obvious displacements in the z-direction for our samples have been observed (data not shown). Hence, we will only analyze, for simplicity, the displacement along the x-axis to study the deviation from affine behavior. Neglecting the displacements in the z- and y-directions which are perpendicular to the direction of shear, might underestimate the non-affine measurements, but would not affect the dependence of affinity with strain.

3.5. Non-affine parameter

The non-affine property of the gels is quantified by the deviation of bead displacements from those for affine deformation as:

$$S = \sqrt{\frac{1}{N}\sum_{i=1}^{N}\left(\frac{d_i - z_i\gamma}{z_i\gamma}\right)^2}, \tag{1}$$

where d_i is the displacement for the ith bead located at z_i when the sample has a macroscopic strain value of γ. For an affine deformation, the strain is uniformly distributed in the gel,

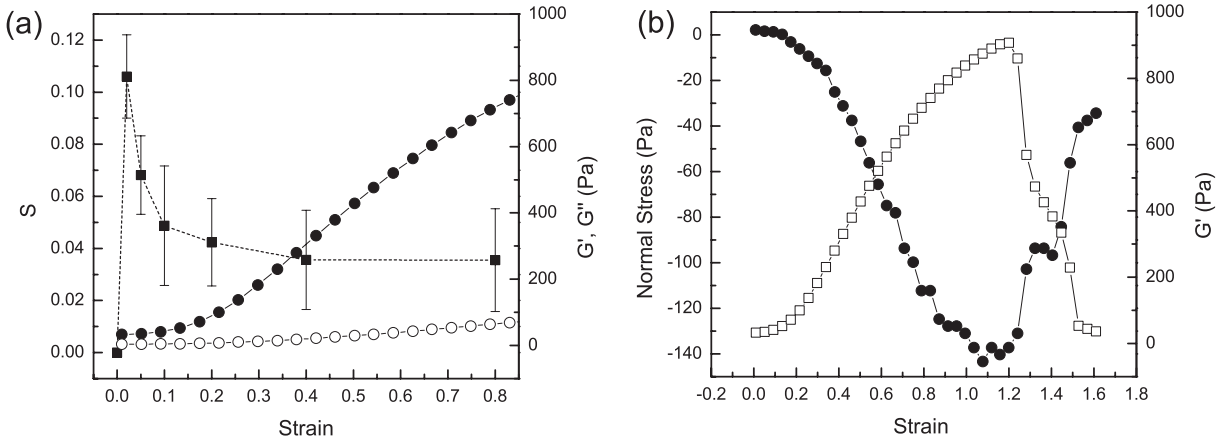

Figure 5. Overlay of S and normal stress with plots of non-linear elasticity. (a) G' (solid circles) increases as a function of strain show strain stiffening of fibrin. S value (solid square) decreases as strain increases indicating that the gel become more affine at higher strain values where strain-stiffening has been observed. (b) Magnitude of negative normal stress (solid circles) has also been observed to increase with increasing strain.

i.e. γ is the same for every bead in equation (1). Under a simple shear strain along the x-direction, a bead located at (x_i, y_i and z_i) in the unstrained gel will displace to a new location (x_i', y_i' and z_i') as

$$\begin{pmatrix} x_i' \\ y_i' \\ z_i' \end{pmatrix} = \begin{pmatrix} 1 & 0 & \gamma_i \\ 0 & 1 & 0 \\ 0 & 0 & 1 \end{pmatrix} \begin{pmatrix} x_i \\ y_i \\ z_i \end{pmatrix}, \tag{2}$$

where γ_i is the strain for this bead. The displacement of the bead induced by the strain is then $d_i = x_i' - x_i = \gamma_i z_i$. Therefore, S is 0 for an affine deformation, since $\gamma_i = \gamma$. For non-affine deformation, the strain is not uniform across the sample, i.e. γ_i is not necessarily equal to γ. Hence, S is non-zero and increases monotonically with a larger degree of non-affinity.

The non-affinity parameter S is plotted as a function of strain in figure 5(a). When the strain is zero, there is no deformation, and the measured S value is zero. There is a sharp increase in S when the strain increases to 2%. After that, S decreases continuously, indicating that the network becomes more and more affine. It is also worth noting in figure 5 that the deviation from affine deformation becomes small at strain values where the gels start to show strain-stiffening behavior.

Computer simulations of semi-flexible filaments in 2D [10, 13, 23, 24] provide models in which non-affine deformations are observed at small strains, and the deformation becomes increasingly affine with increasing strain. Simulation results suggest that the low stiffness of cross-linked semiflexible networks under small strain originates from bending of the semiflexible filaments. At high strains, the stretching response of individual filaments contributes more to the network stiffness. Rearrangements of the network that govern the transition from a bending-dominated response at small strains to a stretching-dominated response at high strains cause the non-affine deformation of gels. Once the stretching sets in, the network becomes more and more affine. The magnitudes of S for fibrin gels shown in figure 5

are not simply related to similar values derived from the 2D simulations, but are small compared to values derived for very disperse networks of very stiff filaments.

Negative normal stress has been ascribed to the asymmetric force-elongation relation of semi-flexible polymers that leads to an imbalance between forces resisting elongation compared to compression of the end-to-end vectors of the filaments between network junctions [25]. In an isotropic network, the number of filaments being stretched is approximately equal to the number of filaments being compressed. However, since bending contributes less resistance than stretching, a net negative normal stress results. At small strains the normal stress is predicted to depend quadradically on strain, consistent with the data in figure 5(b). At higher strain values, the negative normal stress increases more slowly with increasing strain until the sample fails. Within the range of strains where normal stress is negative, there was no evidence of vertical displacements of the fluorescent beads within the resolution of our measurements.

4. Conclusions

Fibrin networks formed under physiological conditions show properties of strain-stiffening and negative normal stress in accordance with those reported [3, 25] for somewhat more uniform gels formed exclusively by fibrin protofilaments under non-physiological conditions. The non-linear viscoelastic response of fibrin gels at moderate strain coincides with very low magnitudes of non-affinity measures. The deviation from affine deformation for isotropic fibrin gels is significantly different from zero, but less than 0.1 at small strains, and it decreases significantly at higher strains, as the shear modulus increases. Although the relatively high S value at low strain could indicate that applied external stress can induce structural reorganization of the network, which provides an explanation to the non-linear elasticity [10], the low S value at moderate strain values suggests that the assumption of affine deformation is approximately applicable for the strains where strain-stiffening is observed, and supports the use of entropic theories to account for this phenomenon. In a biological context these results also imply that extracellular matrices like fibrin, which are the first scaffold set up during wound healing, have isotropic responses to external deformation on the scale of microns measured in this study, even though the network strands have persistence lengths also near a micron. A typical cell like a fibroblast that would be imbedded in a fibrin gel would therefore be subjected to forces consistent with the macroscopic stress on the tissue. Highly non-affine stress fields within a matrix would appear to require stiffer filaments with larger mesh sizes such as recently shown for collagen gels [26] or non-isotropic distributions in order to achieve spatially ordered stresses that would dictate cell responses on a micron scale.

Acknowledgment

This work was supported by grant DMR05-20020 from the National Science Foundation.

References

[1] Kasai M, Kawashima H and Oosawa F 1960 Structure of f-actin solutions *J. Polym. Sci.* **44** 51–69

[2] Leterrier J F, Kas J, Hartwig J, Vegners R and Janmey P A 1996 Mechanical effects of neurofilament cross-bridges modulation by phosphorylation, lipids, and interactions with f-actin *J. Biol. Chem.* **271** 15687–94

[3] Storm C, Pastore J J, MacKintosh F C, Lubensky T C and Janmey P A 2005 Nonlinear elasticity in biological gels *Nature* **435** 191–4
[4] Janmey P A, McCormick M E, Rammensee S, Leight J L, Georges P C and MacKintosh F C 2007 Negative normal stress in semiflexible biopolymer gels *Nat. Mater.* **6** 48–51
[5] Kreplak L, Bar H, Leterrier J F, Herrmann H and Aebi U 2005 Exploring the mechanical behavior of single intermediate filaments *J. Mol. Biol.* **354** 569–77
[6] Gittes F, Mickey B, Nettleton J and Howard J 1993 Flexural rigidity of microtubules and actin filaments measured from thermal fluctuations in shape *J. Cell. Biol.* **120** 923–34
[7] MacKintosh F C, Kas J and Janmey P A 1995 Elasticity of semiflexible biopolymer networks *Phys. Rev. Lett.* **75** 4425–8
[8] Hinner B, Tempel M, Sackmann E, Kroy K and Frey E 1998 Entanglement, elasticity and viscous relaxation of actin solutions *Phys. Rev. Lett.* **81** 2614
[9] Kroy K and Frey E 1997 Dynamic scattering from solutions of semiflexible polymers *Phys. Rev.* E **55** 3092
[10] Onck P R, Koeman T, van Dillen T and van der Giessen E 2005 Alternative explanation of stiffening in cross-linked semiflexible networks *Phys. Rev. Lett.* **95** 178102
[11] Satcher R L Jr and Dewey C F Jr 1996 Theoretical estimates of mechanical properties of the endothelial cell cytoskeleton *Biophys. J.* **71** 109–18
[12] Liu J, Koenderink G H, Kasza K E, MacKintosh F C and Weitz D A 2007 Visualizing the strain field in semiflexible polymer networks: strain fluctuations and nonlinear rheology of f-actin gels *Phys. Rev. Lett.* **98** 198304
[13] Didonna B and Lubensky T 2005 Nonaffinity and nonlinearity in random elastic networks *Phys. Rev.* E **72** 066619
[14] Weisel J W 2004 The mechanical properties of fibrin for basic scientists and clinicians *Biophys. Chem.* **112** 267–76
[15] Gerth C, Roberts W W and Ferry J D 1974 Rheology of fibrin clots. II. Linear viscoelastic behavior in shear creep *Biophys. Chem.* **2** 208–17
[16] Shah J V and Janmey P A 1997 Strain hardening of fibrin gels and plasma clots *Rheol. Acta* **36** 262–8
[17] Wang L Z, Gorlin J, Michaud S E, Janmey P A, Goddeau R P, Kuuse R, Uibo R, Adams D and Sawyer E S 2000 Purification of salmon clotting factors and their use as tissue sealants *Thromb. Res.* **100** 537–48
[18] Michaud S E 2002 Purification of salmon thrombin and its potential as an alternative to mammalian thrombins in fibrin sealants *Thromb. Res.* **107** 245–54
[19] Langer B G, Weisel J W, Dinauer P A, Nagaswami C and Bell W R 1988 Deglycosylation of fibrinogen accelerates polymerization and increases lateral aggregation of fibrin fibers *J. Biol. Chem.* **263** 15056–63
[20] Crocker J C and Grier D G 1996 Methods of digital video microscopy for colloidal studies *J. Colloid Interface Sci.* **179** 298
[21] Rothwell S W, Reid T J, Dorsey J, Flournoy W S, Bodo M, Janmey P A and Sawyer E 2005 A salmon thrombin-fibrin bandage controls arterial bleeding in a swine aortotomy model *J. Trauma* **59** 143–9
[22] Ju Y E, Janmey P A, McCormick M E, Sawyer E S and Flanagan L A 2007 Enhanced neurite growth from mammalian neurons in three-dimensional salmon fibrin gels *Biomaterials* **28** 2097–108
[23] Head D A, Levine A J and MacKintosh F C 2003 Deformation of cross-linked semiflexible polymer networks *Phys. Rev. Lett.* **91** 108102
[24] Head D A, Levine A J and MacKintosh F C 2003 Distinct regimes of elastic response and deformation modes of cross-linked cytoskeletal and semiflexible polymer networks *Phys. Rev.* E **68** 061907
[25] Levental I, Georges P C and Janmey P A 2007 Soft biological materials and their impact on cell function *Soft Matter* **1** 299–306
[26] Chandran P L and Barocas V H 2006 Affine versus non-affine fibril kinematics in collagen networks: theoretical studies of network behavior *J. Biomech. Eng.* **128** 259–70